ISSN 0036-0244, Russian Journal of Physical Chemistry A, 2019, Vol. 93, No. 2, pp. 324–332. © Pleiades Publishing, Ltd., 2019.

PHYSICAL CHEMISTRY OF NANOCLUSTERS AND NANOMATERIALS

Nano Molecular Motor of Azo Antibiotics on Edge-Carboxylated Graphene: A UV and Visible-Switchable Sensors[1]

Majid Monajjemi[a,*]

[a]*Department of Chemical Engineering, Central Tehran Branch, Islamic Azad University, Tehran, Iran*

**e-mail: Maj.monajjemi@iauctb.ac.ir*

Received March 20, 2018

Abstract—In this work, halogenated azobenzene and alpha cyclodexterin (αCD) are simulated as an axle and a wheel respectively, while the edge carboxylated graphene sheet (ECG) is a stopper. Azobenzene onto αCD and combination with ECG can be used such a non-covalent system for photo-isomer-controlled machine. It has been exhibited a new system of molecular motor which works like a hinge motion, and has introduced as light-driven molecular hinges. The αCD ring in the system can be reversibly switched through irradiation of wide range of UV and visible lights. Various sensors can be simulated to predict a model for applying the drug delivery of those antibiotics which cannot be used through straight injection.

Keywords: rotaxane, molecular motor, edge-carboxylated graphene, switchable sensor

DOI: 10.1134/S0036024419020183

INTRODUCTION

Up to now a large diversity of molecular motors such as catenanes and rotaxanes have been synthesized by scientists and researchers [1–3]. Molecular motors are able for a rotational motion in one direction and most of them have been synthesized based on temperature, pressure, pH, light and chemical reaction properties. Recently, various molecular machines are subject to both researches and nano biological activities in viewpoint of energies, cyclic process, types of motion and finally the ways of monitoring as an operating system. These systems are categorized and works as molecular shuttle, molecular propeller, molecular tweezers and molecular switches. A molecular switch works as a system which can reversibly change among a few stable states (mostly two states) which might change and shift in terms of pH, UV–visible photons, increase or decrease of temperature, electricity currents and the presence of a ligand. Recently, artificial molecular motors and machines are designed based on rotaxanes which its name derives from the "*rota*" (a Latin word) and "*axis*" for wheel and axle [1], respectively. Rotaxanes are generally compounded of a molecule (axle-like) surrounded [1] by a macro molecular-ring (rota) and interrupted by a bulky group or a flat sheet as stopper to prevent disassembling [2]. In this work, azobenzene and alpha cyclodexterin (αCD) are simulated as an axle and a wheel respectively, while the carboxylated graphene (G-COOH) sheet is a stopper (Fig. 1). Azobenzene onto αCD can be used such a complex system for photo-isomer-controlled machine [3]. So, rational combination of carboxylated graphene and rotaxanes might present a new research way, given this fact which the presentation of rotaxanes onto carboxylated graphene sheets has not been accomplished previously. In this study, it has been reported a construction of photo-switchable-a-CD based on G-COOH. For achieving photo-switched [4] in this machine, the system has been designed with two stopper-sides including G-COOH and dumb-bell-shaped components with pentahalobiphenyl moiety (Figs. 1, 2).

The αCD, which has hydrophobic cavities, serves as a host for forming an exclusive system with the azobenzene axle including pentahalobiphenyl moiety that acts as a stopper in the end of one side. The system was then attached onto the surface of G-COOH through a sulfur atom and thus, G-COOH acts as the second stopper on the other side of the system. The αCD in the machine over the G-COOH surface can move back and forth along the azobenzene axle between the dumbbell components driven by *cis–trans*-isomerization of the azobenzene segment upon alternating irradiation [4] with UV–visible light (Scheme 1).

cis–trans-ISOMERIZATION OF AZOBENZENE

cis–trans-Isomerization of azobenzene has been used for many functional [5] molecules with applications in photonics for several chemical systems. In this study, we exhibited a new system of molecular motor which works like a hinge motion, and has introduced as light-driven molecular hinges [6]. The characteris-

[1] The article is published in the original.

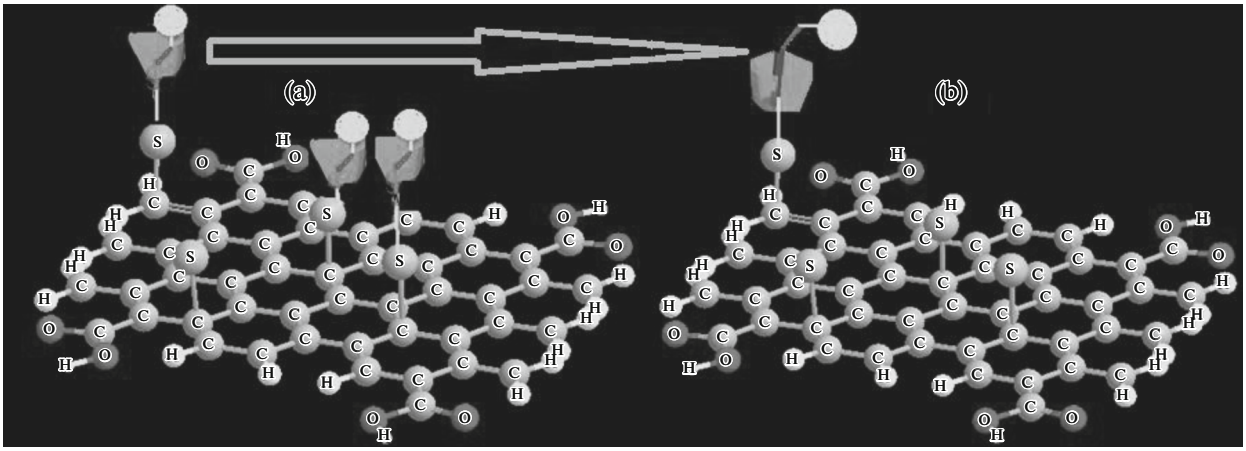

Scheme 1. The schematic presentation of the *trans*- to *cis*-isomerization of the αCD-Azo-ECG molecular machine.

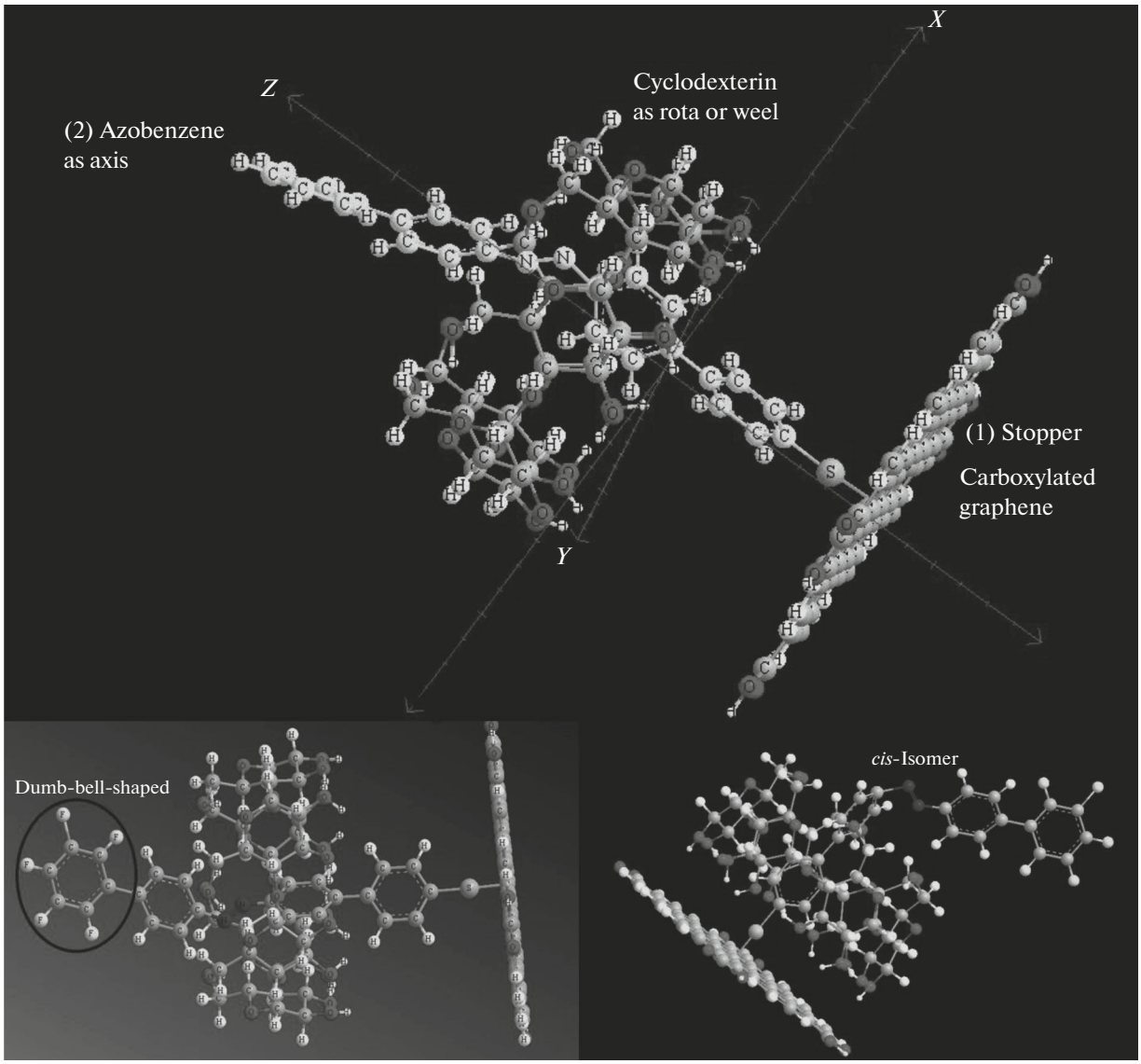

Fig. 1. Optimized of the molecular motor including *cis*- and *trans*-isomers of azobenzene with pentafluorophenyl substituent.

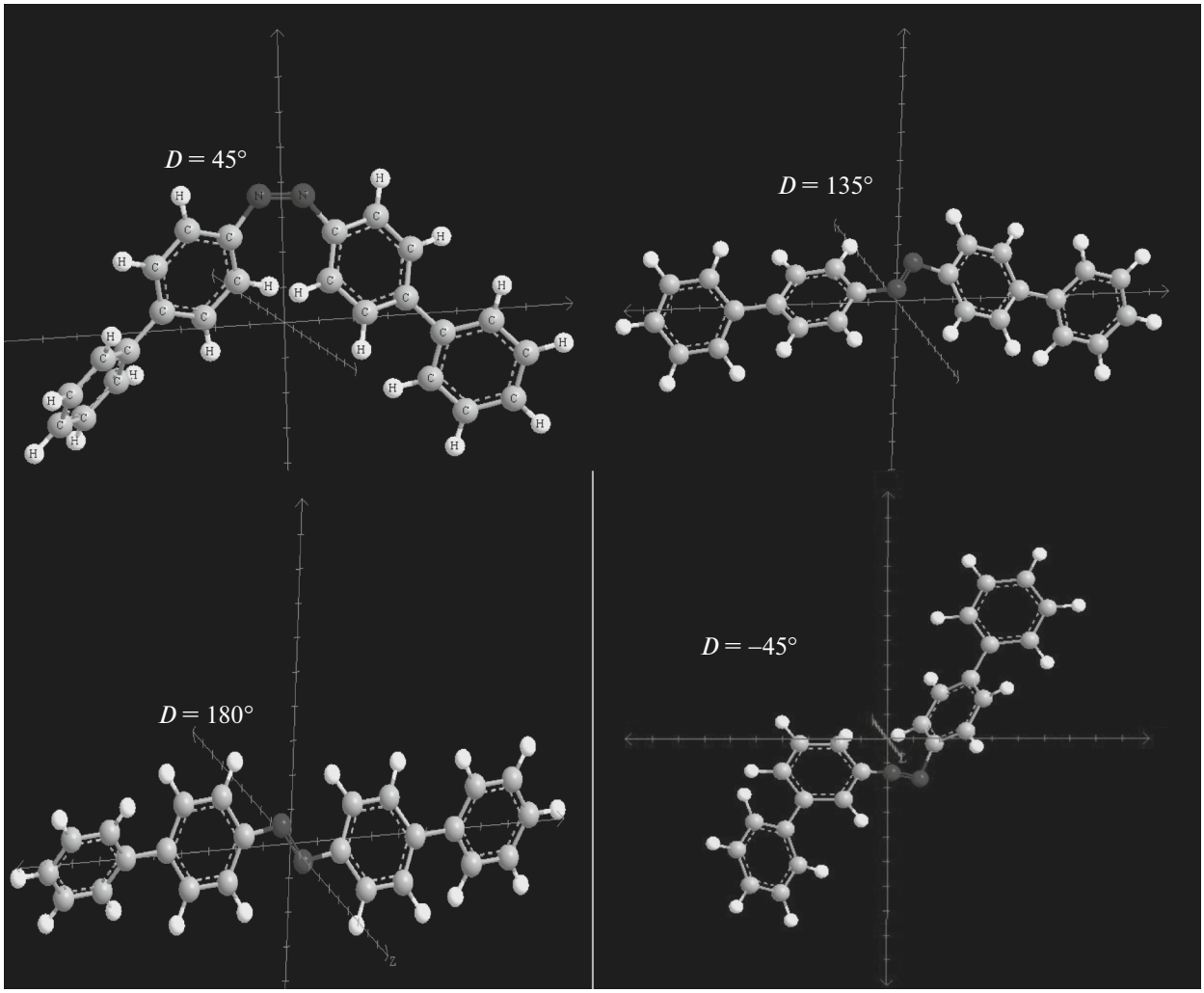

Fig. 2. Various dihedral conformational of azobenzene in several torsions degree ($D = -45°$, 45°, 135°, and 180°).

tic [7] formation of a hinge-like molecule includes two planes which are attached to their edge sides through an axel; the motion of the hinge causes a conversion between close and open states. We have exhibited that the UV–Vis spectrum of our machine for the F-Azo-αCD-functionalized GO has a strong absorption band at 124.95 nm, which is corresponded to the π–π* transition in the *trans*-azobenzene unit and the absorption disappeared after irradiation with UV-C light which indicates that the system is impressed by the *trans*–*cis*-changing. It might be noted that benzene has three aromatic $\pi \rightarrow \pi^*$ transitions; two *E*-bands at 180 and 200 nm and one *B*-band at 255 nm.

COMPUTATIONAL DETAILS

Each part of the machine including 3 sections of ECG, αCD, and Azo has been optimized using ab initio with DFT calculations individually (Fig. 3). Whole of the edge-carboxylated Graphene (ECG) including αCD and Azo axis has been calculated with QM/MM methods and the systems are accomplished with semi empirical methods. In my study, differences of force fields are debated through comparing density and energies with OPLS and AMBER force fields. In addition, a Hyper-Chem professional release 7.01 program has been applied for some additional keywords such as PM3MM, PM6 (pseudo = lanl2).

The final parameterization of *cis*–*trans*-isomerization of azobenzene was computed using SCF calculations in order to find the optimal starting geometries, as well as the difference energies for these conformational structures (Figs. 2, 3). The DFT with the van der Waals densities functional was investigated for modeling of exchange-correlation estimation. All optimization of edge-carboxylated graphene layers were performed by GAMESS-US package [8]. The accurate calculations performed using m062x, m06-L, and m06 for *cis*–*trans*-conformations. The m062x, m06-L, and

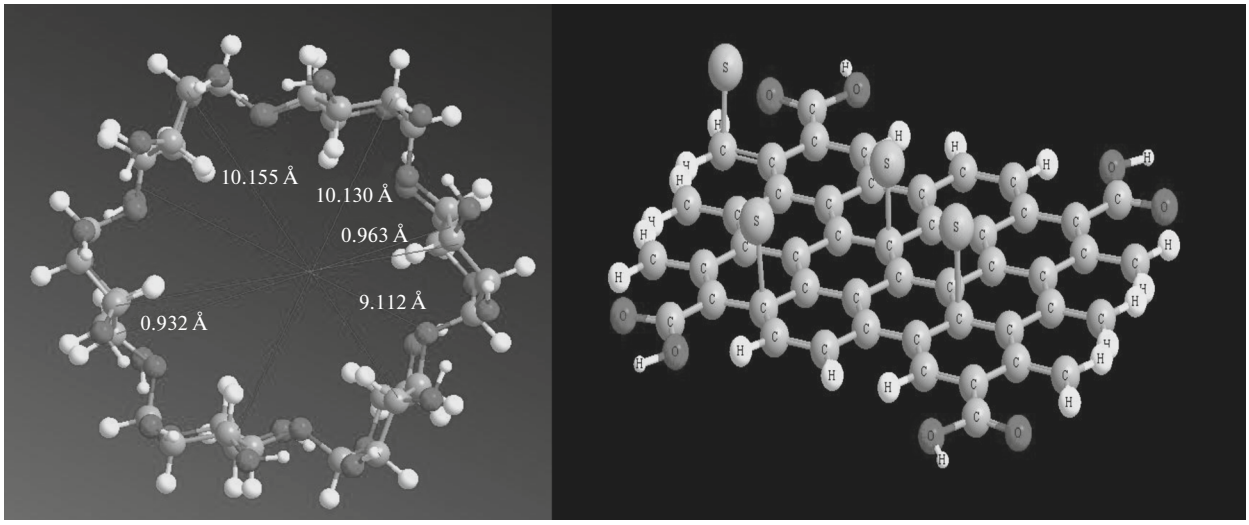

Fig. 3. Optimized alpha-cyclodexterin and optimized edge-carboxylated graphene (ECG).

m06-HF methods have a suitable correspondence in non-bonded calculations between two isomers [9].

For non-covalent interactions between αCD and azobenzene with pentahalophenyl moiety, the ONIOM methods including 3 levels of high (H), medium (M), and low (L) calculations have been done. DFT methods were used for the high (H) layer and the semi empirical method of pm6 and Pm3MM was used for the medium and low layers, respectively.

The electrostatic potentials and charges transfer were also estimated using the Merz–Kollman–Singh [10], chelp [11], and chelp-G [12]. The charge calculation method based on the molecular-electrostatic potentials (MESP) fitting are not well-fixed for treating larger systems whereas some of the innermost atom are located far away from the point at which the MESP is computed. The representative atomic charge for a molecule might be calculated as expectation values over several conformations. The interaction energies among various situations of azobenzene inside αCD were calculated in all items according to the equation:

$$\Delta E_i, \text{ eV} = \{E_{\text{sys}} - (E_{\text{ECG}} + E_{\alpha\text{CD}} + E_{\text{Azo}})\} + E_{\text{BSSE}}, \quad (1)$$

where the ΔE_i is the energy of the systems for various conformations of Azo inside αCD.

Several physical properties such as electron densities, values of orbital wave-functions, electron spin densities, electron localization function (ELF), localized orbital locator (LOL defined by Becke and Tsirelson), total electrostatic potential (ESP), as well as the exchange-correlation densities, and the average local ionization energies (for two *cis–trans*-isomers**)** using the Multifunctional Wave-function analyzer have been also calculated for sulfur bridge [13–15]. This molecular machine has been simulated based on a few fundamental properties such as ELF, LOL, non-bonded interactions and structures of stator and rotor motors which have been investigated in my previous works [16–23].

RESULTS AND DISCUSSION

The light sensor rotaxanes arrays on the ECG surfaces are able to increase the hybrid with new properties. In this work, ECG is used as the carboxylic acid units from the graphene sheet and the covalent immobilization of the UV and Visible-switchable Rotaxane which is a template-directed of a rational combination as the molecular motor (Fig. 1). In contrast to the previous works [24, 25], the sulfide covalent (Fig. 1) instead of van der Waals interactions functionalization are beneficial to enhance the chemical stabilities of the Rotaxane-functionalized ECG hybrid.

In this study, the azobenzene axis and some of its derivation were designed including halogens, with a diphenyl unit acting as a stopper at one side and the S-ECG's bridge at the other side. In this model, a wavelength of 513 nm has been resulted for the Azo system (Table 1) which has a good agreement with the experimental result in the visible region [24]. In the F-Azo case, the mentioned UV–visible wavelength of the Rotaxane-functionalized ECG has an absorption (at 124.95 nm), which is characteristic of the $\pi \rightarrow \pi^*$ transition of the *trans*-azobenzene isomer. Hong Yan and coworkers [24] exhibited experimentally, that an absorption peak is appeared in the UV–Vis spectrum, which corresponds to the 4-propargyloxybenzene unit on the GO surface and experimentally approves our theoretical work. In this work, only one stereoisomer in which the secondary side of the αCD rings faces the diphenyl stopper was demonstrated (Fig. 1). In addition, it has been presented that the αCD ring in the Rotaxane can move back and forth between the Azo-axis and its derivation units upon *trans–cis*-isomeriza-

Table 1. The $\Delta E_{trans-cis}$ for various halogens machine as the photo-switchable sensor (E is total energy of motor including (axle, wheel, and Stopper)) (Hartree)

Axle systems	$-E$, Hartree	$\Delta E_{transt-cis}$, kcal/mol	Wavelength, nm; frequency (THZ)	Region of photo-switchable sensor
C_6F_5-azobenzene (*cis*)	561.669633	228.82	124.95, 2399	Ultra Violet C (UVC)
C_6F_5-azobenzene (*trans*)	561.305785			
C_6Cl_5-azobenzene (*cis*)	552.0813416	730.50	39.14, 7659	Extreme Ultra Violet (EUV)
C_6Cl_5-azobenzene (*trans*)	550.9172141			
C_6Br_5-azobenzene (*cis*)	549.7902484	709.39	40.30, 7438	Extreme Ultra Violet (EUV)
C_6Br_5-azobenzene (*trans*)	548.6597573			
Azobenzene (*cis*)	532.934125	55.73	513.0, 584	Visible
Azobenzene (*trans*)	532.8453108			

Table 2. The physical properties of sulphur-ECG bond in various system of Azo derivation in a same machine

Axle systems	Lumo/Homo gap, kcal/mol		Electron density	Electron spin density	ELF, LOL	Local information entropy	$U(r)$, $K(r)$	$\frac{\sum_1^{248} \text{LIE}}{N}$, ESP
	α orbitals	β orbitals	$\sum_1^{248}$ atoms	$\sum_1^{248}$ atoms				
Azo-*cis*	3.48	1.23	0.478	0.369	0.177, 0.419	0.741	0.272, –0.120	0.779, –0.647
Azo-*trans*	4.30	10.43	0.586	0.184	0.102, 0.318	0.891	–0.118, –0.529	0.815, –0.619
Br-Azo-*cis*	3.35	5.51	0.482	0.201	0.164, 0.127	0.721	–0.187, –0.122	0.776, –0.676
Br-Azo-*trans*	0.30	5.22	0.588	0.524	0.304, 0.174	0.864	–0.196, –0.119	0.813, –0.644
Cl-Azo-*cis*	2.35	0.03	0.482	0.592	0.213, 0.145	0.720	–0.149, –0.121	0.776, –0.672
Cl-Azo-*trans*	2.813	2.40	0.588	0.120	0.308, 0.175	0.864	–0.194, –0.119	0.813, –0.643
F-Azo-*cis*	3.48	1.23	0.478	0.370	0.177, 0.419	0.715	0.272, –0.120	0.779, –0.655
F-Azo-*trans*	4.27	10.41	0.585	0.183	0.102, 0.318	0.860	–0.118, –0.529	0.815, –0.628

tion were controlled by different wavelengths (Fig. 2, Table 1). Besides, the *trans–cis*- and *cis–trans*-isomers of the Azo-systems lead to two points whose results are confirmed experimentally by [24] and theoretically the results exhibited two wavelengths around 513 and 124.95 nm for two systems of H-Azo and F-Azo machines in visible and UV regions, respectively. As it can be seen in the Fig. 1 and Scheme 1, the αCD ring in the Rotaxane unit is primarily located at the *trans*-position, which is obviously far away from the surface of the ECG and then αCD ring moves towards ECG sheet position. In contrast of previous position, the *trans–cis*-transformation of the Azo system appears on upper wavelength, so the action of the αCD in forth and back wheel along the Azo-axis depends on two states of Rotaxane-functionalized ECG which is intrinsically useful for any light-sensors.

In extra calculations, the other halogen atoms (Br and Cl) were replaced instead of five hydrogens in the last phenyl ring which interestingly the wavelength for the molecular machine shifts to down range in the UVC (for F) and EUV (for Cl and Br) regions. In this work, our focus is partially based on the electron density, Hamiltonian kinetic energy $K(r)$, potential energy density $U(r)$, LOL, ELF, and average local ionization energy of the sulfur atom when the halogens have been replaced one by one in other side of Azo system. The electron density (e/Bohr^3) has been defined as:

$$\rho(r) = \eta_i |\varphi_i(r)|^2 = \sum_i \eta_i \left| \sum_l C_{l,i}\chi_i(r) \right|^2, \qquad (2)$$

where the η_i denotes orbital's occupation number and φ_i is related orbital wave function. As it can be seen in the Table 2, the amount of these parameters are much more different for sulphur atom in the system of Cl-Azo and Br-Azo compare to H-Azo machine while the data for F-Azo is similar to H-Azo. One of the reasons is the different covalent atomic radius of chlorine with hydrogen (99 – 53 = 46 pm) and bromine (114 – 53 = 58 pm) which are larger than the fluorine (71 – 53 = 28 pm). Bader [26] has found that the areas with big electron localization might have large values of Fermi-hole. Becke and Edgecombe suggested electron localization function (ELF) for relation between spin pair probability with the Fermi hole [27]:

$$\text{ELF}(r) = \frac{1}{1 + [D(r)/D_0(r)]^2}, \qquad (3)$$

where

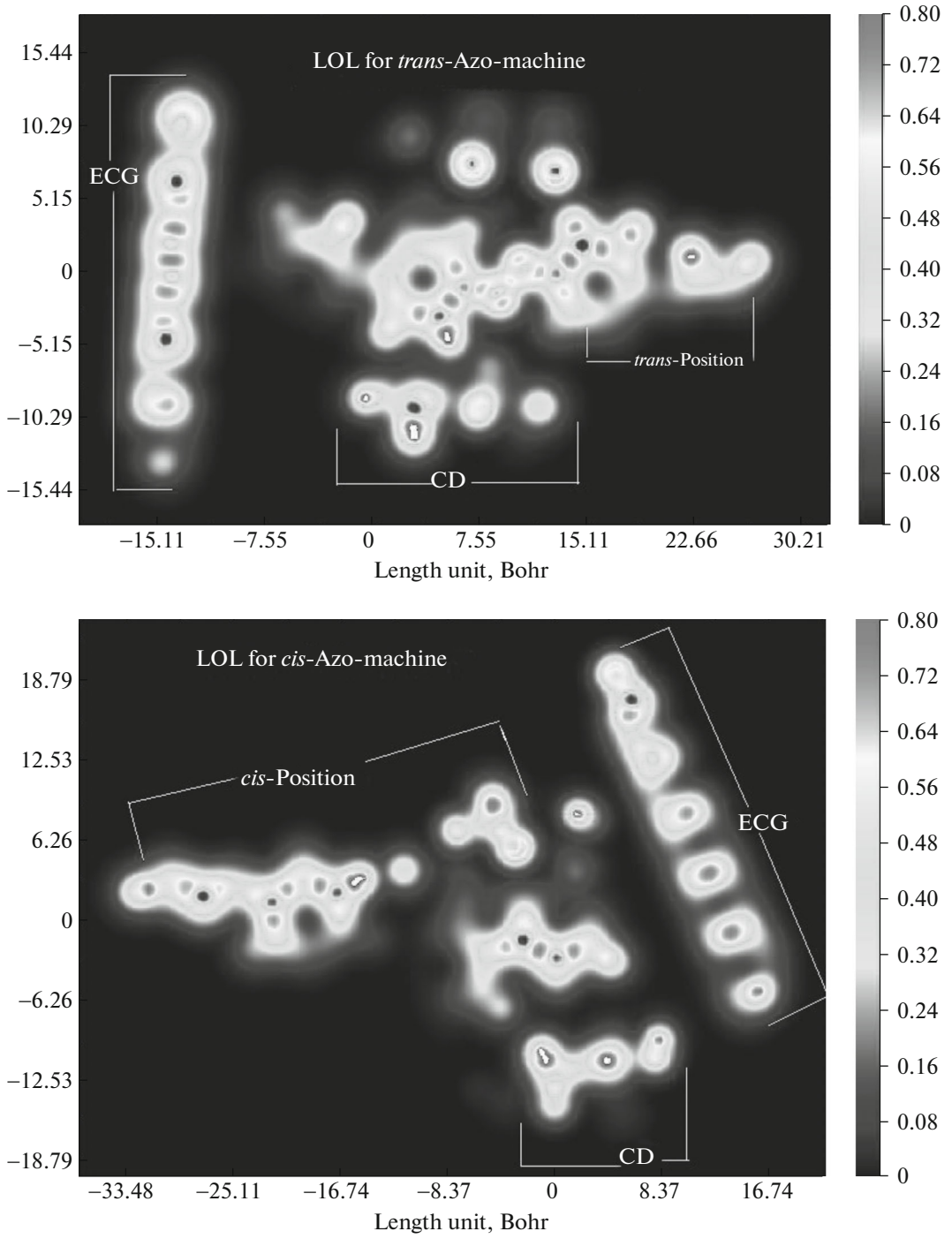

Fig. 4. Color-field map of LOL for *cis*- and *trans*-isomers of Azo machine which indicates the geometries, value of LOL and distances.

$$D(r) = \frac{1}{2}\sum_i \eta_i |\nabla\varphi_i|^2 - \frac{1}{8}\left[\frac{|\nabla\rho_\alpha|^2}{\rho_\alpha(r)} + \frac{|\nabla\rho_\beta|^2}{\beta(r)}\right], \quad (4)$$

$$D_0(r) = \frac{3}{10}(6\pi^2)^{\frac{2}{3}}\left[\rho_\alpha(r)^{\frac{5}{3}} + \rho_\beta(r)^{\frac{5}{3}}\right]. \quad (5)$$

As it can be seen in the Table 2, the ELF value for sulfur is larger than LOL in the systems of Cl-Azo and Br-Azo (both for *cis* and *trans*) while this amount is shorter for H-Azo and F-Azo. ELF gives a relative localization and varied between the range of [0, 1]. A large amount of ELF up to 1 describes that electrons are completely localized and the large amounts indicate lone pair, a covalent bond or inner shells of the

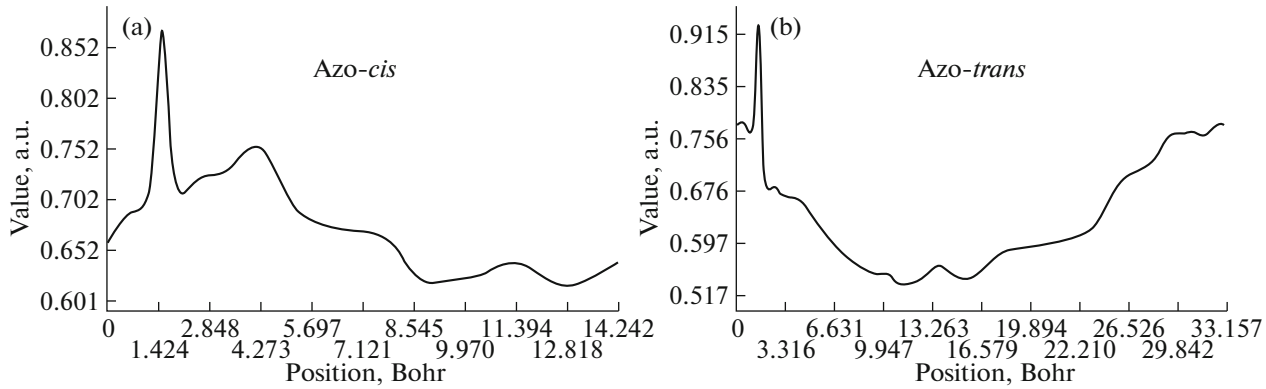

Fig. 5. Average local ionization energy for H-Azo-machines.

atoms. In the Table 2, the ELF in all systems is less than 0.5 which means the electron is not localized for the S-ECG's bridge and makes flexibility for moving the Rotaxane back and forth between the Azo-axis and its derivation units which were controlled by different wavelengths. This flexibility for *trans*-H-Azo and *trans*-F-Azo is more than *trans*-Br-Azo and *trans*-Cl-Azo machines due to spatial barrier of Cl and Br compare to F.

Savin et al. [28] have investigated the ELF in viewpoint of kinetic energies, which indicated that $D(r)$ gives the excess kinetic energy densities caused by Pauli repulsion, while $D_0(r)$ can be thought-out as Thomas–Fermi kinetic energies. As it can be seen in Tables 1, 2, the difference of Hamiltonian kinetic energies between *cis* and *trans* isomers for the F-Azo is more than the Cl-Azo and Br-Azo machines, meanwhile potential energy density for *cis*-H-Azo and *cis*-F-Azo is positive while for the other systems is negative. It causes that the *cis*-Br-Azo and *cis*-Cl-Azo molecular motors cannot move to back and forth in the larger wave lengths (visible and UVC) (Table 2) while they act in higher energies or shorter wave lengths (EUV) compare to *cis*-H-Azo and *cis*-F-Azo molecular motors.

LOL formalism is defined by Schmider and Becke in the [29]:

$$\mathrm{LOL}(r) = \frac{\tau(r)}{1+\tau(r)}, \qquad (6)$$

where

$$(r) = \frac{D_0(r)}{\frac{1}{2}\sum_i \eta_i |\nabla\varphi_i|^2}.$$

LOL has a similar statement compared to ELF but the LOL (Fig. 4) gives more definitive and explicit images than ELF. Based on Eq. (6), LOL can be demonstrated in kinetic energy path in contrast of ELF; small (large) LOL magnitude generally appears in border regions of localized orbital because the gradient of orbital wave-function is large (small) in this region. In Table 2 the LOL is larger than the ELF for both *cis* and *trans* of H-Azo and F-Azo systems while it is smaller for Cl-Azo and Br-Azo which confirms the above interpretation.

The data of molecular electrostatic potential and average local ionization energies are listed in the last column of Table 2 and Fig. 5. ESP has been widely used for prediction of molecular recognitions and intermolecular interaction of S-ECG bonds. In other words, the total electrostatic potentials (ESP) measure the electrostatic interaction between sulfur point charges and the ECG surface. All data are approximately equal and negative (Table 2) and a negative value implies that the current position is dominated by nuclear charges (not electronic charges), so they are independent of halogens radii and depends only to ECG surface properties.

The distances between ECG and αCD for halogens-Azo along the S-Azo axis (Fig. 6, Table 3) are not equal in the right and left sides of the machines which indicate that the axis has a deviation from the ECG surface. The changing of these deviations caused the αCD in the machine over the G-COOH surface easily moved back and forth along the azobenzene axle. As it can be seen in the Table 3, the changing of these distances in the left side (in contrast the right side) is approximately equal which indicates that this movement is monotonous in one direction.

Table 3. Displacement distances from *trans* to *cis* of CD between two dumbbell components, Å

Displacements	Right side	Left side
H-Azo-machine	4.46	4.82
F-Azo-machine	4.45	4.80
Cl-Azo-machine	4.39	4.80
Br-Azo-machine	4.36	4.79

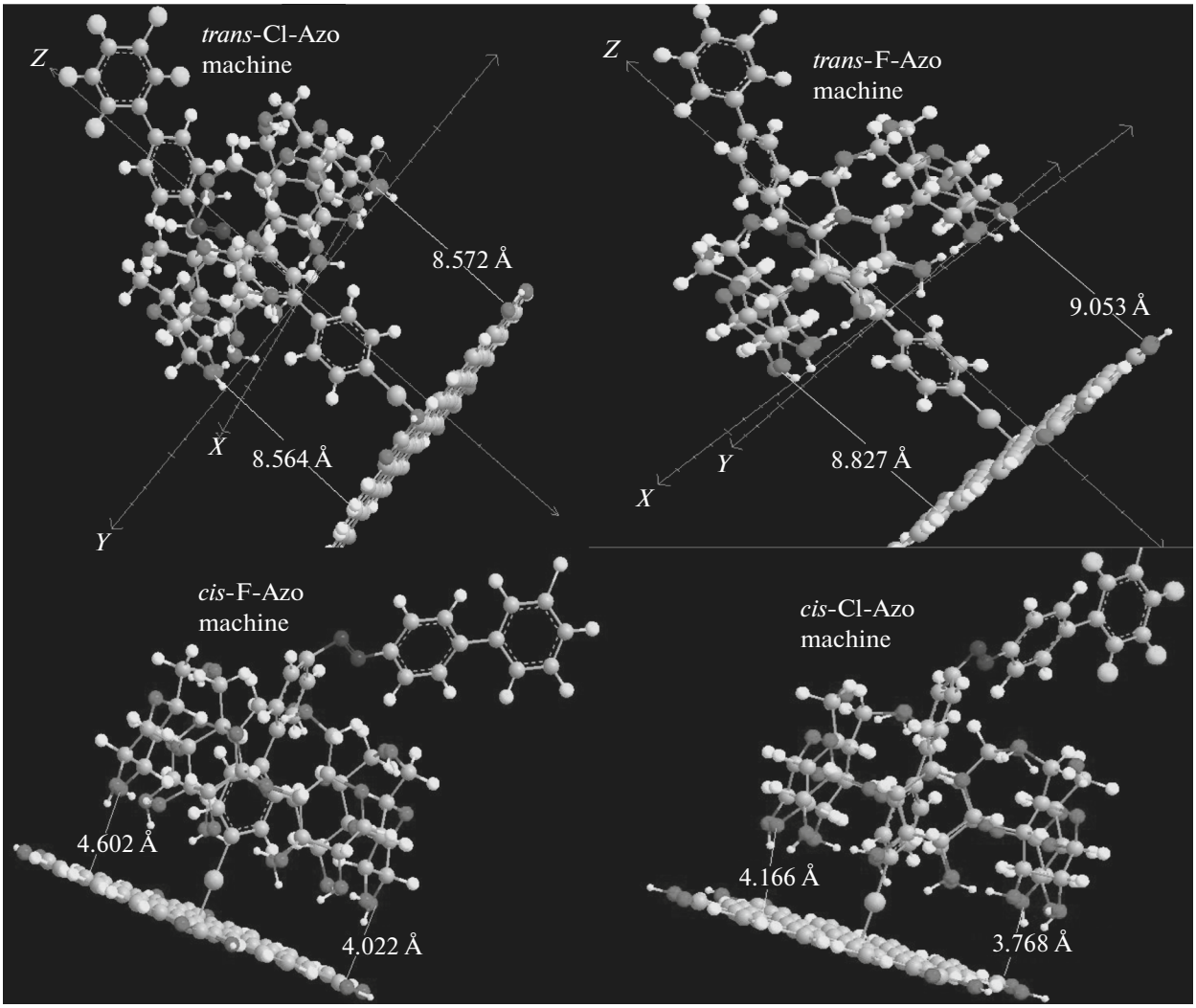

Fig. 6. The distances between ECG and αCD for F-Azo and Cl-Azo machines along the S-Azo axis.

CONCLUSION

We have successfully modeled a system to introduce light-sensor of αCD-based rotaxanes onto the surface of ECG. The αCD ring in the system can be reversibly switched through irradiation of wide range of UV and visible lights. Through changing the size of dumb-bell in one side (with halogens in this work) and fixing it in another side of ECG surface, various systems in wide range of UV and visible sensors can be simulated to predict a model for any further experiments of designing molecular machines which are suitable for drug delivery in nano technology subjects.

REFERENCES

1. V. Balzani, A. Credi, and M. Venturi, *A Journey into the Nano World* (Wiley-VCH, Weinheim, 2004). doi 10.1002/3527601600.ch1
2. J.-P. Sauvage and C. Dietrich-Buchecker, *Molecular Catenanes, Rotaxanes, and Knots* (Wiley-VCH, Weinheim, 1999).
3. H. Yan, C. Teh, S. Sreejith, L. Zhu, A. Kwok, W. Fang, X. Ma, K. T. Nguyen, V. Korzh, and Y. L. Zhao, Angew. Chem. Int. Ed. **51**, 8373 (2012).
4. P. R. Ashton, R. Ballardini, V. Balzani, A. Credi, K. R. Dress, E. Ishow, C. J. Kleverlaan, O. Kocian, J. A. Preece, N. Spencer, J. F. Stoddart, M. Venturi, and S. Wenger, Chem. Eur. J. **6**, 3558 (2000). doi 10.1002/1521-3765(20001002)6
5. S. Shinkai, T. Ogawa, T. Nakaji, Y. Kusano, and O. Manabe, Tetrahedron Lett. **47**, 4569 (1979).
6. A. D. Hamilton and D. van Engen, J. Am. Chem. Soc. **109**, 5035 (1987). doi 10.1021/ja00250a052
7. S. Shinkai, G.-X. He, T. Matsuda, A. D. Hamilton, and H. S. Rosenzweig, Tetrahedron Lett. **30**, 5895 (1989). doi 10.1016/S0040-4039(01)93499-9
8. M. W. Schmidt, K. K. Baldridge, J. A. Boatz, S. T. Elbert, M. S. Gordon, J. H. Jensen, S. Koseki, N. Matsunaga,

K. A. Nguyen, et al., J. Comput. Chem. **14**, 1347 (2004). doi 10.1002/jcc.540141112

9. Y. Zhao and D. G. Truhlar, Theor. Chem. Acc. **120**, 215 (2008). doi 10.1007/s00214-007-0310-x
10. B. H. Besler, K. M. Merz, and P. A. Kollman, J. Comput. Chem., No. 11, 431 (1990). doi 10.1002/jcc.540110404
11. L. E. Chirlian and M. M. Francl, J. Comput. Chem., No. 8, 894 (1987). doi 10.1002/jcc.540080616
12. G. M. Brneman and K. B. Wiberg, J. Comput. Chem., No. 11, 361 (1990).
13. T. Lu and F. Chen, Acta Chim. Sin. **69**, 2393 (2011).
14. T. Lu and F. J. Chen, Mol. Graph. Model **38**, 314 (2012).
15. T. Lu and F. Chen, J. Comput. Chem., No. 33, 580 (2012). doi 10.1002/jcc.22885
16. M. Monajjemi, V. S. Lee, M. Khaleghian, B. B. Honarparvar, and F. F. Mollaamin, J. Phys. Chem. C **114**, 15315 (2010). doi 10.1021/jp104274z
17. M. Monajjemi, Struct Chem. **23**, 551 (2012). doi 10.1007/s11224-011-9895-8
18. M. Monajjemi and J. E. Boggs, J. Phys. Chem. A **117**, 1670 (2013). dx.doi.org/10.1021/jp312073q
19. M. Monajjemi, Theor. Chem. Acc. **134**, 77 (2015). doi 10.1007/s00214-015-1668-9
20. M. Monajjemi, J. Mol. Model. **20**, 2507 (2014). doi 10.1007/s00894-014-2507-y
21. M. Monajjemi, Biophys. Chem. **207**, 114 (2015). doi 10.1016/j.bpc.2015.10.003
22. M. Monajjemi, Chem. Phys. **425**, 29 (2013). doi 10.1016/j.chemphys.2013.07.014
23. M. Monajjemi, J. Mol. Liq. **230**, 461 (2017). doi 10.1016/j.molliq.2017.01.044
24. H. Yan, L. Zhu, X. Li, A. Kwok, X. Pan, and Y. Zhao, Asian J. Org. Chem. **1**, 314 (2012). doi 10.1002/ajoc.201200102
25. A. G. Cheetham, M. G. Hutchings, T. D. Claridge, and H. L. Anderson, Angew. Chem. **118**, 1626 (2006); Angew. Chem. Int. Ed. **45**, 1596 (2006).
26. R. F. W. Bader, *Atoms in Molecule: A Quantum Theory* (Oxford Univ. Press, Oxford, 1990).
27. A. D. Becke and K. E. Edgecombe, J. Chem. Phys. **92**, 5397 (1990). http://dx.doi.org/10.1063/1.458517
28. A. Savin, O. Jepsen, J. Flad, O. K. Andersen, H. Preuss, and H. G. von Schnering, Angew. Chem. Int. Ed. Engl. **31**, 187 (1992).
29. B. H. Besler, K. M. Merz, and P. A. Kollman, J. Comput. Chem. **11**, 431 (1990). http://dx.doi.org/10.1002/jcc.540110404